J Mater Sci (2007) 42:6895–6900
DOI 10.1007/s10853-006-1473-x

Stresses in superconductor during oxygenation

Ladislav Ceniga

Received: 4 November 2006 / Accepted: 19 December 2006 / Published online: 30 April 2007

Abstract The paper deals with an analytical model of stresses acting in the superconductor YBCO during an oxygenation process to transform the tetragonal lattice of the non-superconductive phase $YBa_2Cu_3O_{7-x_0}(x_0 = 0.9)$ to the orthorhombic lattice of the superconductive phase $YBa_2Cu_3O_7$. Accordingly, the oxygenation-induced stresses originate as a consequence of the difference in dimensions of the crystalline lattices. Additionally, critical temperature of the oxygenation process with regard to a crack formation in the superconductor YBCO is derived.

Introduction

The superconductor $YBa_2Cu_3O_7$–Y_2BaCuO_5 (123–211) represents a matrix–particle system acted by stresses originating during a cooling process as a consequence of the difference in thermal expansion coefficients of the phases 123 and 211 [1], as well as during an oxygenation process of the single-grain bulk phase 123. The oxygenation process transforms the tetragonal lattice of the non-superconductive phase $YBa_2Cu_3O_{7-x_0}$ ($x_0 = 0.9$) to the orthorhombic lattice of the superconductive phase $YBa_2Cu_3O_7$. The superconductive phase is required because of its zero resistance against electric current. Accordingly, the stresses originating during the oxygenation process are a consequence of different dimensions of the tetragonal and orthorhombic lattices, as experimentally investigated in [2]. Finally, this paper represents an analytical contribution to the experimental results.

L. Ceniga (✉)
Institute of Materials Research, Slovak Academy of Sciences, Watsonova 47, Košice 043 53, Slovak Republic
e-mails: lceniga@imr.saske.sk; lceniga@yahoo.com; lceniga@hotmail.com

Analytical model

Cell model

As presented in Ref. [2], the oxygenation process, applying to the sample YBCO in a form of the cylindrical pellet shown in Fig. 1a ($D = 35$, $h = 20$ [mm]), is realized in cylindrical holes with the radius R_1, the length h and the inter-cylinder distance $2R_3$. With regard to an analytical model, this system with the finite dimension D is replaced by an infinite system ($D \to \infty$) divided into cylindrical cells with parameters R_1, R_3, h (see Fig. 1b). Consequently, the oxygenation-induced stresses are investigated within the cylindrical cell, considering the boundary condition $(\sigma_r)_{r=R_3} = 0$ for the radial stress σ_r. Resulting from the system infinity, analytical models of the oxygenation-induced stresses in a certain cylindrical cell are identical with those in any cylindrical cell.

In spite of the fact that an influence of the matrix between the cylindrical cells is not considered, the same approach, presented in [3], is used in case of an analytical model of thermal stresses originating in a matrix–particle system consisted of periodically distributed spherical particles with the radius R_1 and the inter-particle distance $2R_3$, where the spherical particles are embedded in an infinite matrix divided into spherical cells with the radius R_3. Consequently, an influence of the matrix between the spherical cells is not considered, and the same boundary condition $(\sigma_r)_{r=R_3} = 0$ is used to result in more than satisfactory theoretical results compared with experimental observation.

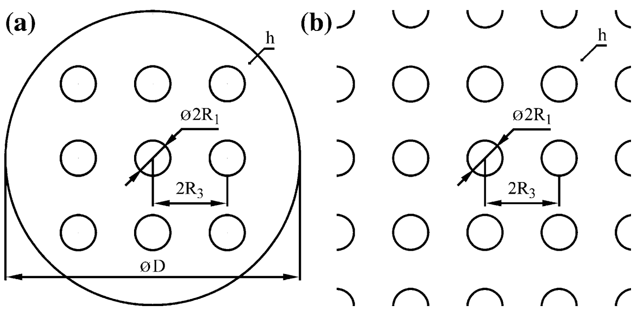

Fig. 1 Shape of the sample of the single-grain bulk 123 phase (**a**) as experimentally investigated in [2], and the system (**b**) considered regarding the analytical model

Cylinders A and B

The sample of the single-grain bulk phase 123 is oxygenated at the different temperature T to result in the different oxygen concentration C in a crystalline lattice of the 123 phase. Consequently, the different concentration C results in the different crystalline lattice dimensions a_1 and a_3 in the plane x_1x_2 and along the axis x_3 (see Fig. 2), respectively. An initial state of the phase 123 is thus characterized by the parameters a_{10}, a_{30} related to the temperature T_0 resulting in C_0, where T_0 is simultaneously final temperature of a crystal growth process of the phase 123 [2, 4]. Performing the oxygenation process at the temperature $T < T_0$, the parameters a_{10}, a_{30} are transformed to $a_1 \neq a_{10}$, $a_3 \neq a_{30}$ corresponding to C at the radii R_1, respectively, where $C \neq C_0$.

Additionally, with regard to simplification of the analytical model, the oxygen concentration C is assumed to be constant within the cylinder with the radii R_1 and $R_2 < R_3$. Accordingly, the cylindrical cell consists of the cylinders A and B with the radii R_1, R_2 and R_2, R_3 (see Fig. 2), respectively. The cylinders A and B are thus represented by the phases $YBa_2Cu_3O_7$ and $YBa_2Cu_3O_{7-x_0}$ ($x_0 = 0.9$) with the crystalline lattice dimensions a_1, a_3 and a_{10}, a_{30}, respectively, where a_1, a_3 are assumed not to be functions of the spherical variables $r \in \langle R_1, R_2\rangle$, $\varphi \in \langle 0, 2\pi\rangle$.

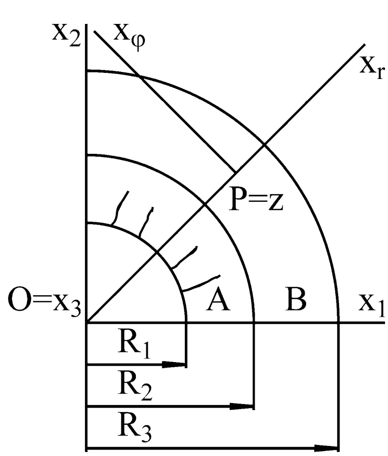

Fig. 2 The hollow cylinders A and B with the radii $R_1 < R_2 < R_3$, and the axes x_r, x_ϕ and $z = c\| x_3$ in the general point P, along which the radial, tangential and longitudinal stresses σ_r, σ_ϕ and σ_z act, respectively, and radial cracks with the length h formed in the cylinder A provided that $\sigma_{\phi\ A} > 0$ and on the condition $(\sigma_{\varphi A})_{r=R_1} > \sigma_{fr}$ (see section ''Stresses in cylinders A and B'')

Stresses in cylinders A and B

Considering the system consisted of the hollow cylinders A and B of the 123 phase and with the radii $R_1 < R_2 < R_3$ (see Fig. 2), the radial, tangential and longitudinal stresses σ_r, σ_ϕ and σ_z are investigated in the general point P along the axis x_r, x_ϕ and z, respectively, where x_r, $x_\phi \subset x_1x_2$; $z\| x_3$. With regard to parameters of the phase 123 [1], the isotropic and anisotropic planes x_1x_2, x_1x_3 and x_2x_3, respectively, correspond to the tetragonal lattice, and the coordinate r along the axis x_r is related to the cylinders A, B for $r \in \langle R_1, R_2\rangle$, $r \in \langle R_2, R_3\rangle$, respectively. With regard to isotropy of the plane x_1x_2, we get

$$\frac{\partial u_r}{\partial \varphi} = 0, \tag{1}$$

and consequently the shear strain $\varepsilon_{r\phi} = \varepsilon_{r\phi} = (1/r)\ (\partial u_r/\partial \phi) = 0$ [5] results in the shear stress $\sigma_{r\phi} = \sigma_{\phi\ r} = 0$, where u_r is displacement of an infinitesimal cylindrical part of the system along the axis x_r, and the angle $\varphi = \angle(x_1, OP)$.

Additionally, the displacements u_r and u_z, the latter along the axis z, are assumed to be independent on the variables z and r, respectively, as derived by the condition

$$\frac{\partial u_r}{\partial z} = \frac{\partial u_z}{\partial r} = 0, \tag{2}$$

and consequently the shear strain $\varepsilon_{rv} = (\partial u_r/\partial z) + (\partial u_z/\partial r) = 0$ [5] results in the shear stress $\sigma_{rv} = \sigma_{v\ r} = 0$. Finally, along with Eqs. (1), (2), the strains ε_{zA}, ε_{zB} along the axis z are connected with the condition

$$\varepsilon_{zA} = \varepsilon_{zB} = \frac{a_3 - a_{30}}{a_{30}}. \tag{3}$$

Considering the dimension changes a_1–a_{10}, a_3–a_{30} to originate in crystalline lattices of the cylinder A only, the cylinders A and B tend to exhibit the radii $R_2 + R_2[(a_1–a_{10})/a_{10}]$ and R_2, respectively, where R_2/a_{10} represents a number of crystalline lattices with the dimension a_{10} related to the distance R_2. The radius change $R_2(a_1–a_{10})/a_{10}$ induces the compressive or tensile radial stress $p_2 > 0$ or $p_2 < 0$ acting on the A–B boundary, respectively. The radial stress p_2 results in the radial strains $(\varepsilon_{rA})_{r=R_2}, (\varepsilon_{rB})_{r=R_2}$ in the cylinders A, B, respectively. The A–B boundary thus exhibits the radius

$$R_{AB} = R_2 + R_2\frac{a_1 - a_{10}}{a_{10}} + R_2(\varepsilon_{rA})_{r=R_2} = R_2 + R_2(\varepsilon_{rB})_{r=R_2}, \tag{4}$$

and consequently we get the condition

$$(\varepsilon_{rB})_{r=R_2} - (\varepsilon_{rA})_{r=R_2} = \frac{a_1 - a_{10}}{a_{10}} \tag{5}$$

used for the determination of the radial stress p_2. The Cauchy's equations have the forms [5]

$$\varepsilon_r = \frac{\partial u_r}{\partial r}, \tag{6}$$

$$\varepsilon_\varphi = \frac{u_r}{r}, \tag{7}$$

$$\varepsilon_z = \frac{\partial u_z}{\partial z}, \tag{8}$$

and consequently the compatibility equation (9) to result from Eqs. 6, 7, and the equilibrium equation (10) related to the axis x_r [5] have the forms

$$\varepsilon_r - \varepsilon_\varphi - r\frac{\partial \varepsilon_\varphi}{\partial r} = 0, \tag{9}$$

$$\sigma_\varphi = \sigma_r + r\frac{\partial \sigma_r}{\partial r}, \tag{10}$$

where $\partial\sigma_\phi/\partial\phi = 0$ and $\partial\sigma_z/\partial z = 0$ results from equilibrium equations related to the axes x_ϕ and z due to $\sigma_{r\phi} = \sigma_{\phi\ r} = 0$ and $\sigma_{rv} = \sigma_{v\ r} = 0$, respectively. Finally, the Hooke's laws corresponding to the tetragonal lattice are derived as [5]

$$\varepsilon_r = s_{11}\sigma_r + s_{12}\sigma_\varphi + s_{13}\sigma_z, \tag{11}$$

$$\varepsilon_\varphi = s_{12}\sigma_r + s_{11}\sigma_\varphi + s_{13}\sigma_z, \tag{12}$$

$$\varepsilon_z = s_{31}(\sigma_r + \sigma_\varphi) + s_{33}\sigma_z, \tag{13}$$

and the elastic modulus s_{ij} (i, j = 1, 2, 3) [5] has the form

$$s_{ij} = \frac{\delta_{ij} - \mu_j(1 - \delta_{ij})}{E_i}, \quad i,j = 1,2,3, \tag{14}$$

where E_i and μ_j are the Young's modulus and the Poisson's number, and δ_{ij} = 0, 1 for $i \neq j$, $i = j$ is the Kronecker's symbol, respectively. With regard to Eqs. 10, 13, the stress σ_z is derived as

$$\sigma_z = \frac{1}{s_{33}}\left[\varepsilon_z - s_{31}\left(2\sigma_r + r\frac{\partial\sigma_r}{\partial r}\right)\right]. \tag{15}$$

With regard to $\partial\varepsilon_z/\partial r = (\partial/\partial r)(\partial u_z/\partial z) = (\partial/\partial z)(\partial u_z/\partial r) = 0$ (see Eqs. 2, 8), considering Eqs. 10–12, 15, the compatibility equation (9) is transformed to the form

$$r\frac{\partial^2\sigma_r}{\partial r^2} + 3\frac{\partial\sigma_r}{\partial r} = 0, \tag{16}$$

and consequently, assuming the radial stress in the form $\sigma_r = Cr^\lambda$, we get

$$\sigma_r = C_1 + \frac{C_2}{r^2}, \tag{17}$$

where the coefficients C_1, C_2 are determined from boundary conditions. Considering the boundary conditions

$$(\sigma_{rA})_{r=R_1} = 0, \tag{18}$$

$$(\sigma_{rA})_{r=R_2} = (\sigma_{rB})_{r=R_2} = -p_2, \tag{19}$$

$$(\sigma_{rB})_{r=R_3} = 0, \tag{20}$$

the stresses in the cylinders A and B have the forms

$$\sigma_{rA} = -\frac{p_2}{1 - r_{12}^2}\left[1 - \left(\frac{R_1}{r}\right)^2\right], \quad r_{12} = \frac{R_1}{R_2} \in \langle 0, 1), \tag{21}$$

$$\sigma_{\varphi A} = -\frac{p_2}{1 - r_{12}^2}\left[1 + \left(\frac{R_1}{r}\right)^2\right], \tag{22}$$

$$\sigma_{zA} = \frac{1}{s_{33A}}\left(\frac{2s_{31A}p_2}{1 - r_{12}^2} + \varepsilon_{zA}\right), \tag{23}$$

$$\sigma_{rB} = -\frac{p_2}{1 - r_{32}^2}\left[1 - \left(\frac{R_3}{r}\right)^2\right], \quad r_{32} = \frac{R_3}{R_2} > 1, \tag{24}$$

$$\sigma_{\varphi B} = -\frac{p_2}{1 - r_{32}^2}\left[1 + \left(\frac{R_3}{r}\right)^2\right], \tag{25}$$

$$\sigma_{zB} = \frac{1}{s_{33B}}\left(\frac{2s_{31B}p_2}{1 - r_{32}^2} + \varepsilon_{zB}\right). \tag{26}$$

With respect to Eqs. 5, 12, 21–26, the radial stress p_2 is derived as

$$p_2 = \frac{1}{c_1 - c_2}\left[\frac{a_1 - a_{10}}{a_{10}} + \frac{a_3 - a_{30}}{a_{30}}\left(\frac{s_{13A}}{s_{33A}} - \frac{s_{13B}}{s_{33B}}\right)\right]. \tag{27}$$

and the coefficients c_1, c_2 have the forms

$$c_1 = s_{12A} + \frac{1}{1-r_{12}^2}\left[s_{11A}\left(1+r_{12}^2\right) - \frac{2s_{13A}s_{31A}}{s_{33A}}\right], \tag{28}$$

$$c_2 = s_{12B} + \frac{1}{1-r_{32}^2}\left[s_{11B}\left(1+r_{32}^2\right) - \frac{2s_{13B}s_{31B}}{s_{33B}}\right], \tag{29}$$

where a_{10}, a_1 and a_{30}, a_3 are lattice parameters along the axis x_1 and x_3, related to the temperature T_0, $T < T_0$, respectively.

Critical temperature of oxygenation process

Provided that the tangential stress $\sigma_{\phi A}$ is tensile, then for $\sigma_{\phi A} > 0$; on the condition $\left(\sigma_{\varphi A}\right)_{r=R_1} > \sigma_{fr}$; and with regard to $\sigma_{\phi A} - r$ representing a decreasing function of the variable $r \in \langle R_1, R_2 \rangle$; radial cracks with the length h in the cylinder A are formed from a surface with the radius R_1 during the oxygenation process, where σ_{fr} is critical stress with respect to crack formation. To avoid the crack formation, the condition

$$\left(\sigma_{\varphi A}\right)_{r=R_1} \le \sigma_{fr}, \tag{30}$$

being accordingly required to be fulfilled, is transformed, after substitution of Eqs. 22, 27 to Eq. 30, to the temperature condition

$$T \ge T_{op}. \tag{31}$$

Consequently, assuming the linear temperature dependence

$$a_{1+2i} = k_{1+2i}T + q_{1+2i}, \quad i = 0, 1, \tag{32}$$

the critical temperature of the oxygenation process, T_{op}, related to the temperature T_0, has the form

$$T_{op} = \frac{c_3 c_4 - c_5}{c_6} \tag{33}$$

and the coefficients c_3–c_6 are derived as

$$c_3 = (k_1 T_0 + q_1)(k_3 T_0 + q_3), \tag{34}$$

$$c_4 = 1 + \frac{s_{13A}}{s_{33A}} - \frac{s_{13B}}{s_{33B}} - \frac{\sigma_{fr}}{2}(c_1 - c_2)\left(1 - r_{12}^2\right), \tag{35}$$

$$c_5 = q_3(k_1 T_0 + q_1)\left(\frac{s_{13A}}{s_{33A}} - \frac{s_{13B}}{s_{33B}}\right) + q_1(k_3 T_0 + q_3), \tag{36}$$

$$c_6 = k_3(k_1 T_0 + q_1)\left(\frac{s_{13A}}{s_{33A}} - \frac{s_{13B}}{s_{33B}}\right) + k_1(k_3 T_0 + q_3), \tag{37}$$

where $a_{1+2i0} = (a_{1+2i})_{T=T\_0}$ $(i = 0,1)$.

Oxygenation-induced stresses in phase 123

With regard to the temperature dependence (32), the crystalline lattice dimensions a_1 and a_3 of the phase 123 in the plane x_1x_2 and along the axis x_3, respectively, are shown in Fig. 3 [4] as functions of the oxygenation temperature T, where a_1, a_3 are measured at the room temperature $T_r = 20$ °C, and consequently changes of a_1, a_3 due to thermal expansion in the temperature interval $\langle T_r, T \rangle$ are neglected.

Considering material and lattice parameters of the phase 123 presented in Table 1, the radial, tangential, axial stresses, σ_{rA}, $\sigma_{\phi A}$, σ_{zA} and σ_{rB}, $\sigma_{\phi B}$, σ_{zB} (see Eqs. 21–26) in the layers A and B, respectively, for the radii $R_1 = 0.5$, $R_2 = 1$, $R_3 = 1.5$, for the initial temperature $T_0 = 900$ °C and the oxygenation temperature $T = 400$ °C are shown in Fig. 4. The temperature $T_0 = 900$ °C and $T = 400$ °C to result in $a_{10} = 3.865$, $a_{30} = 11.833$ and $a_1 = 3.856$, $a_3 = 11.696$ $[10^{-10}$ m] (see Eq. 32; Table 1) is the same as considered within the experimental results published in [2, 4], respectively. Additionally, the nomograms $\sigma_{\phi A}$–r_{12}–r_{32}, σ_{rA}–r_{12}–r_{32} at the radii $r = R_1$, $r = R_2$ in the layer A to exhibit tendency to release the oxygenation-induced stress loading by radial crack formation (see Figs. 2, 7), are presented in Figs. 5, 6. Finally, the dependencies in Figs. 5, 6 are not asymptotic for $r_{12} \to 1$ due to reduction of the term 1–r_{12}^2 in fractions of Eqs. 21, 22, 27–29.

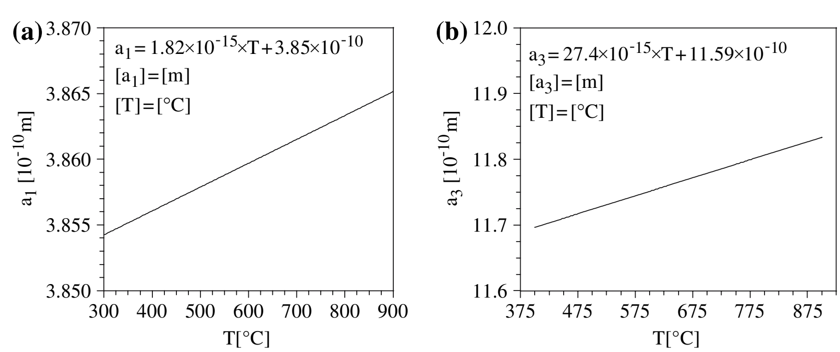

Fig. 3 The crystalline lattice dimensions a_1 (**a**) and a_3 (**b**) of the phase 123 in the plane x_1x_2 and along the axis x_3 (see Fig. 2), respectively, as functions of the oxygenation temperature T, where a_1, a_3 are measured at the room temperature $T = 20$ °C [4]

Table 1 Material and lattice parameters of the 123 phase (see Fig. 3a, b; Eq. 32) [1, 4]

E_1 (GPa)	E_3 (GPa)	μ_1	μ_3	R_1 (10^{-3} m)	R_2 (10^{-3} m)	R_3 (10^{-3} m)	k_1 (10^{-15} m T^{-1})	k_3 (10^{-15} m T^{-1})	q_1 (10^{-10} m)	q_3 (10^{-10} m)
182	143	0.255	0.255	0.5	1	1.5	1.81596	27.3978	3.8488	11.5869

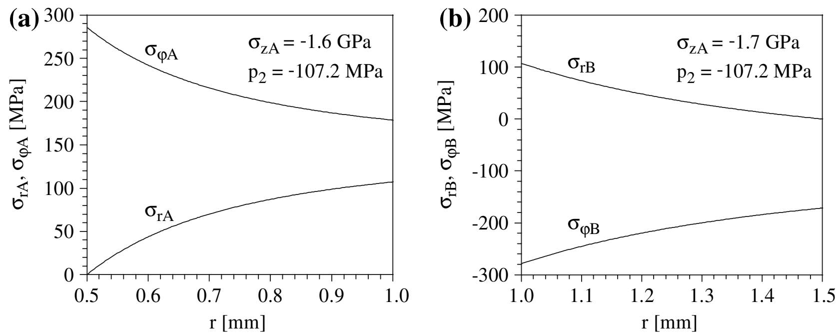

Fig. 4 The radial and tangential stresses σ_{rA}, σ_{rB} and $\sigma_{\phi\ A}$, $\sigma_{\phi\ B}$, along with the axial stresses σ_{zA}, σ_{zB}, acting in the cylinders A, B (see Eqs. 21–26), respectively, with the radii $R_1 = 0.5$ mm, $R_2 = 1$ mm, $R_3 = 1.5$ mm for the temperature $T_0 = 900$, $T = 400$ [°C] (see Eq. 32), where $\sigma > 0$ or $\sigma < 0$ represents tensile or compressive stress, respectively, and p_2 is a radial stress acting on the $A - B$ boundary (see Eq. 27)

Fig. 5 Nomograms of the tensile tangential stress $\left(\sigma_{\varphi A}\right)_{r=R_1} > 0$, acting at the radius $r = R_1$, as functions of the parameters $r_{12} \in \langle 0, 1\rangle$ and $r_{32} > 1$ (see Eqs. 21, 22, 24) for the temperature $T_0 = 900$, $T = 400$ [°C] (see Eq. 32), where $(\sigma_{rA})_{r=R_1} = 0$ (see Eq. 18). The dependence $\left(\sigma_{\varphi A}\right)_{r=R_1} - r_{12} - r_{32}$ for $r_{32} > 5$ is approximately identical to the curve 27 (**b**)

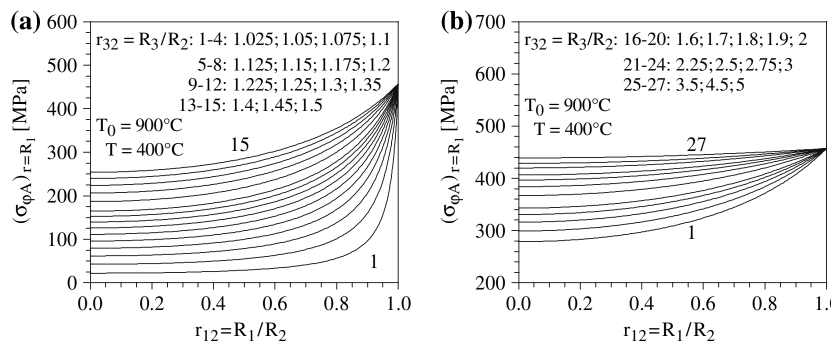

The nomogram T_{op}–r_{12}–r_{32} for the initial temperature $T_0 = 900$ °C, and for the critical stress $\sigma_{fr} = 25$ MPa [4] regarding the radial crack formation is presented in Fig. 7. Resulting from $R_2 = R_2(t)$ as an increasing time-dependent function for $(R_2)_{t=0} = R_1$ [6], the critical temperature T_{op} for $t = 0$ and $t > 0$ is considered for $r_{12} = 1$ and $r_{12} \in \langle 0, 1)$ (see Eq. 21), respectively, with regard to $r_{32} \geq 1$.

To avoid the crack formation, the critical temperature T_{op} is required to be as small as possible in comparison with the initial temperature T_0. Accordingly, a state of the sample YBCO with small radius R_1 (for $r_{12} \to 0$) and high density of the cylindrical holes (for $r_{32} \to 1$) is required, what results in small critical temperature T_{op} as presented in Fig. 7.

Conclusions

Representing a continuation of the paper [2] with experimental results to concern the oxygenation process resulting in a transformation of the tetragonal lattice of the non-superconductive phase $YBa_2Cu_3O_{7-x_0}$ ($x_0 = 0.9$) to the orthorhombic lattice of the superconductive phase $YBa_2Cu_3O_7$, the latter exhibiting zero resistance against electric current and both denoted as the phase 123, main results concerning the analytical model of the oxygenation-induced stresses presented in this paper are as follows:

1. The sample with the finite diameter $D \nrightarrow \infty$ and the height h, containing cylindrical holes with the radius R_1, the length h and the inter-cylinder distance $2R_3$, as shown in Fig. 1a and experimentally investigated in [2], is replaced by the system with $D \to \infty$ shown in Fig. 1b,
2. considering the same approach as presented in [3] to result in sufficiently exact theoretical results, the system is divided into cylindrical cells with the radii R_1, R_3, and consequently the oxygenation-induced stresses are investigated within the cell (see section ''Cell model''),
3. as presented in section ''Cylinders A and B'', with regard to simplification of the analytical model, the

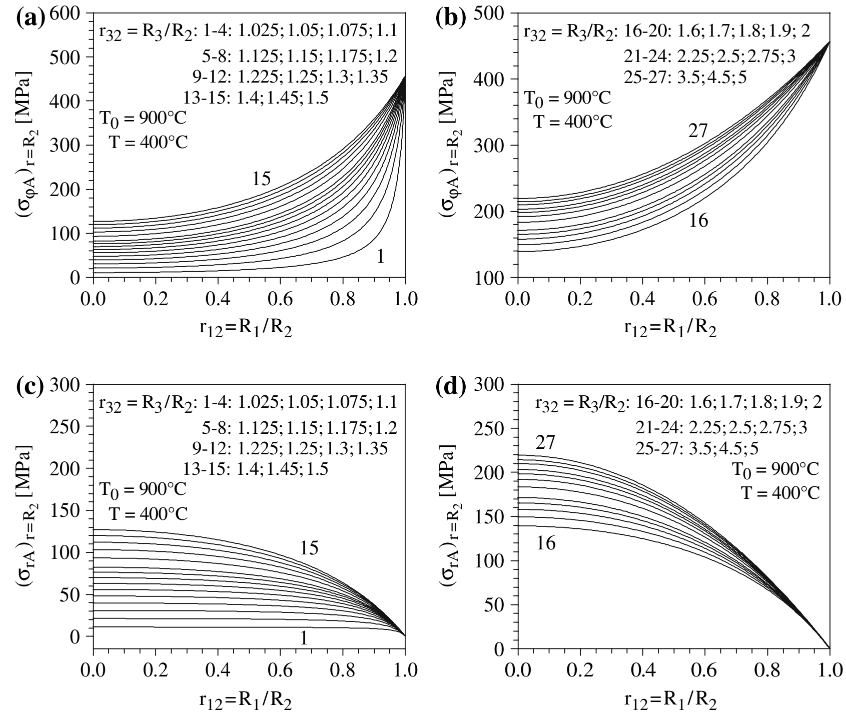

Fig. 6 Nomograms of the tensile tangential and radial stresses, $(\sigma_{\varphi A})_{r=R_2} > 0$ (**a**, **b**) and $(\sigma_{rA})_{r=R_2} = -p_2 > 0$ (*c*,*d*) (see Eq. 19), respectively, acting at the radius $r = R_2$, as functions of the parameters $r_{12} \in \langle 0, 1 \rangle$ and $r_{32} > 1$ (see Eqs. 21, 22, 24, 27) for the temperature $T_0 = 900$, $T = 400$ [°C] (see Eq. 32). The dependencies $(\sigma_{\varphi A})_{r=R_2} - r_{12} - r_{32}$ and $(\sigma_{rA})_{r=R_2} - r_{12} - r_{32}$ for $r_{32} > 5$ are approximately identical to the curve 27 (**b**, **d**)

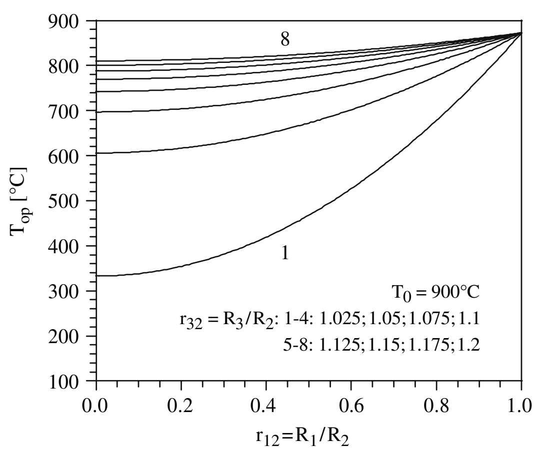

Fig. 7 Nomograms of the temperature T_{op} as a function of the parameters $r_{12} \in \langle 0, 1 \rangle$ and $r_{32} > 1$ (see Eqs. 21, 24, 33), for material and lattice parameters of the 123 phase (see Table 1). The dependence T_{op}–r_{12}–r_{32} for $r_{32} > 1.2$ is approximately identical to the curve 8

cylinder with the radii R_1, R_3 is divided into the cylinders *A* and *B* with the radii R_1, $R_2 < R_3$ and R_2, R_3, and with the constant oxygen concentration *C* and $C_0 \neq C$ to result in the crystalline lattice dimensions a_1, a_3 and $a_{10} \neq a_1, a_{30} \neq a_3$ in the plane x_1x_2, along the axis x_3 (see Fig. 2), respectively,

4. the analytical model of the oxygenation-induced stresses and the condition (30) to avoid the crack formation in the layer *A* acted by the tensile tangential stress $\sigma_{\phi\ A} > 0$ (see Eq. 22) are presented in sections ''Stresses in cylinders *A* and *B*'' and ''Critical temperature of oxygenation process'', along with the critical temperature of the oxygenation process, T_{op}, regarding the crack formation,
5. an application of the analytical model to phase 123 is presented in section ''Oxygenation-induced stresses in phase 123'', along with nomograms of the tangential, radial stresses in the cylinder *A* and the critical temperature, $\sigma_{\phi\ A}$, σ_{rA} and T_{op}, respectively.

Acknowledgements This work was supported by APVV No. COST-0022-06, by the Slovak Grant Agency VEGA (1/1111/04, 2/4062/04, 2/4173/04, 2/4175/04), by NANOSMART, Centre of Excellence, Slovak Academy of Sciences, by Science and Technology Assistance Agency under the Contracts APVT-51-049702, APVV-20-061505, APVV-20-024405, by SICMAC RTN2-2001-00488, by 2003 SO 51/03R8 06 00/03R 06 03-2003, by NENAMAT INCO-CT-2003-510363, by EU 5th FP Project No. GRD1-2000-25352 ''Smart Weld'', by COST Action 536 and COST Action 538, by János Bolyai Research Grant NSF-MTA-OTKA grant—MTA: 96/OTKA: 049953, OTKA 63609.

References

1. Ceniga L, Diko P (2003) Physica C 385:329
2. Diko P, Kračunovsá S, Ceniga L, bierlich J, Zeisberger M, Gawalek W (2005) Supercond Sci Technol 18:1400
3. Mizutani T (1996) J Mater Res 11:483
4. Diko P (2004) Supercond Sci Technol 17:R45
5. Ivančo V, Kubín K, Kostolný K (1994) In: Finite element methodI. Slovak Republic, Elfa Košice, p 36
6. Sedláček V, Králík F, Šejnoha R (1968) In: Diffusion and precipitation processes in metallic systems. Academia Prague, Czech Republic, p 72